



# HHS Public Access

Author manuscript

*Soil Environ Health*. Author manuscript; available in PMC 2023 October 12.

Published in final edited form as:

*Soil Environ Health*. 2023 June ; 1(2): . doi:10.1016/j.seh.2023.100017.

## Fate and distribution of orally-ingested CeO<sub>2</sub>-nanoparticles based on a mouse model: Implication for human health

Xingmao Ma<sup>a,\*</sup>, Xiaoxuan Wang<sup>a</sup>, Lei Xu<sup>b</sup>, Honglan Shi<sup>c</sup>, Hu Yang<sup>b</sup>, Kerstin K. Landrock<sup>d,e</sup>, Virender K. Sharma<sup>f</sup>, Robert S. Chapkin<sup>d,e,\*</sup>

<sup>a</sup> Zachry Department of Civil and Environmental Engineering, Texas A&M University, College Station, TX, 77843, USA

<sup>b</sup> Linda and Bipin Doshi Department of Chemical and Biochemical Engineering, Missouri University of Science and Technology, Rolla, MO, 65409, USA

<sup>c</sup> Department of Chemistry and Center for Research in Energy and Environment, Missouri University of Science and Technology, Rolla, MO 65409, USA

<sup>d</sup> Department of Nutrition, Texas A&M University, College Station, TX, 77843, USA

<sup>e</sup> Program in Integrative Nutrition & Complex Diseases, Texas A&M University, College Station, TX, 77843, USA

<sup>f</sup> Department of Environmental and Occupational Health, Texas A&M University, College Station, TX, 77843, USA

### Abstract

The use of nanoparticles in agrichemical formula and food products as additives has increased their chances of accumulation in humans via oral intake. Due to their potential toxicity, it is critical to understand their fate and distribution following oral intake. Cerium oxide nanoparticle (CeO<sub>2</sub>NP) is commonly used in agriculture and is highly stable in the environment. As such, it has been used as a model chemical to investigate nanoparticle's distribution and clearance. Based on their estimated human exposure levels, 0.15–0.75 mg/kg body weight/day of CeO<sub>2</sub>NPs with different sizes and surface charges (30–50 nm with negative charge and <25 nm with positive charge) were gavaged into C57BL/6 female mice daily. After 10-d, 50% of mice in each treatment were terminated, with the remaining being gavaged with 0.2 mL of deionized water daily for 7-d. Mouse organ tissues, blood, feces, and urine were collected at termination. At the tested levels, CeO<sub>2</sub>NPs displayed minimal overt toxicity to the mice, with their accumulation in various organs being negligible. Fecal discharge as the predominant clearance pathway took less than 7-d regardless of charges. Single particle inductively coupled plasma mass spectrometry analysis

This is an open access article under the CC BY-NC-ND license (<http://creativecommons.org/licenses/by-nc-nd/4.0/>).

\* Corresponding authors. Zachry Department of Civil and Environmental Engineering, Texas A&M University, College Station, TX, 77843, USA. xma@civil.tamu.edu (X. Ma), r-chapkin@tamu.edu (R.S. Chapkin).

#### Declaration of Competing Interest

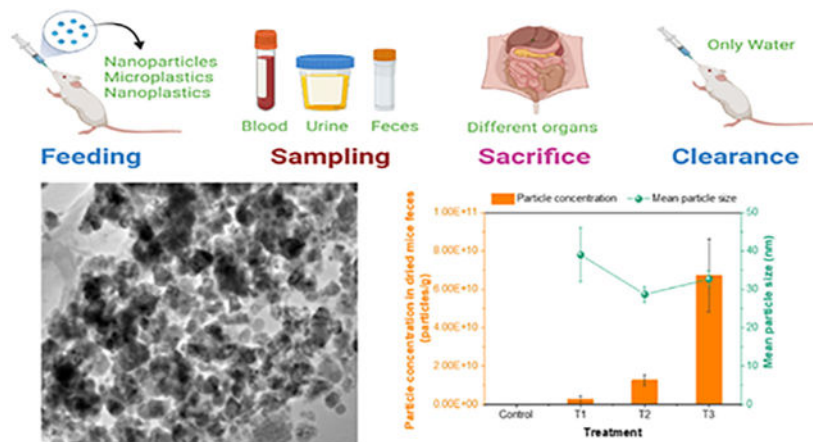
The authors declare that they have no known competing financial interests or personal relationships that could have appeared to influence the work reported in this paper.

Appendix A. Supplementary data

Supplementary data to this article can be found online at <https://doi.org/10.1016/j.seh.2023.100017>.

demonstrated minimal aggregation of CeO<sub>2</sub>NPs in the gastrointestinal tract. These findings suggest that nanoparticle additives >25 nm are unlikely to accumulate in mouse organ after oral intake, indicating limited impacts on human health.

## Graphical Abstract



## Keywords

Cerium oxide nanoparticles; Different size; Oral intake; Different charge; SP-ICP-MS; Environmental impacts

## 1. Introduction

Emulsifiers, artificial sweeteners, and coating and thickening agents are common food additives in western diets to increase shelf life and improve the quality and taste of pre-packaged foods (Chazelas et al., 2020). With the rapid development of nanotechnology, inorganic nanoparticles (NPs) are commonly used in food products, pharmaceutical formulations, and personal care products (McClements and Xiao, 2017). For example, titanium oxide (TiO<sub>2</sub>, E171) NPs are found in >900 food products (Pinget et al., 2019). Silicon oxide NPs (SiO<sub>2</sub>, E551) are the second most common as food additives, with an average adult consuming ~1.8 mg SiO<sub>2</sub>/bw/d (Dekkers et al., 2011). In addition to these intentionally-introduced NPs in food products, our food can be incidentally polluted by NPs accumulated in soils. Therefore, it is important to evaluate the impacts of NPs on human health.

Prolonged consumption of nanoparticle food additives may lead to their accumulation in different organs and cause deleterious effects (Medina-Reyes et al., 2020). However, detailed mechanisms of action are still lacking, and it is not uncommon to find contradictory statements concerning the fate and distribution of food-borne NPs in the literature (Lamas et al., 2020), which is attributed in large part to the challenge of detecting and precisely quantifying NPs and dissolved ions following dissolution. For example, silver and zinc oxide NPs are commonly used in this type of studies, however, it is recognized that these NPs undergo rapid dissolution in the acidic stomach fluid (He et al., 2020). Therefore,

detection of elemental Ag and Zn in different organs cannot conclusively demonstrate NP's accumulation in these organs. If NPs indeed accumulate in different organs, it is also important to have insights into their physicochemical properties and behaviors (e.g., their possible aggregation) in biological tissues, which is lacking in the literature. Fortunately, recent advances in analytical techniques capable of simultaneously characterizing particle size, size distribution and particle concentration in biological samples have occurred in the past few years. Single-particle inductively-coupled plasma-mass spectrometry (SP-ICP-MS) is a popular technology for this purpose, which can simultaneously provide NP size and size distribution, particle number concentration as well as the concentration of their ions.

CeO<sub>2</sub>NP is a popular engineered-NP that has been used in many commercial and agricultural products, making it one of the most likely exposed NPs by humans. CeO<sub>2</sub>NPs is also a major candidate in nanomedicine due to its superoxide dismutase and catalase mimetic activities (Baldim et al., 2018). Indeed, it shows great potential for various human diseases including Alzheimer's disease and obesity (Inbaraj and Chen, 2020). Recently, the investigation of CeO<sub>2</sub>NPs has been extended to oncology, neurology, chronic inflammation and hepatology (Casals et al., 2020). Importantly, CeO<sub>2</sub>NPs are stable under physiological conditions in the gastrointestinal tract. Therefore, CeO<sub>2</sub>NPs is used as a model NP to investigate the fate and distribution of orally-ingested NPs.

Oral ingestion is an important pathway of exposure to inorganic NPs. In spite of many studies, it remains unsettled as to whether orally taken inorganic NPs can pass through the intestinal epithelial barrier and enter the bloodstream and organs. The primary goal of this study was to understand the fate, distribution and clearance of orally-administered CeO<sub>2</sub>NPs and how their properties affect their behavior after oral intake using a mouse model. The results from this study should have some implication regarding the impacts of CeO<sub>2</sub>NPs on human health.

## 2. Materials and methods

### 2.1. Nanoparticle sources and characterization

CeO<sub>2</sub>NPs with different sizes and surface charges from two different sources were obtained. The uncoated CeO<sub>2</sub>NP dispersion with a particle size <25 nm (10% weight in H<sub>2</sub>O) was from Sigma Aldrich (St. Louis, MO) and the particles were positively charged. CeO<sub>2</sub>NPs dispersion of 30–50 nm (20% weight in H<sub>2</sub>O) was from U.S. Research Nanomaterials (Houston, TX) and was negatively charged due to the polyvinylpyrrolidone coating. To verify their properties, the mean nanoparticle size, size distribution and shape were determined using a Tecnai G2 F20 transmission electron microscope (TEM) (FEI). The hydrodynamic size and zeta potential of these particles dispersed in deionized (DI) water at 10 mg/L were measured using a dynamic light scattering instrument (Zetasizer Nano ZS, Malvern Inc., Worcestershire, UK). The crystal structure of CeO<sub>2</sub>NPs was evaluated with a Hitachi H-9500 high resolution (HR)-TEM with a lattice resolution of 0.1 nm and point-to-point resolution of 0.18 nm.

## 2.2. In vivo study design

C57BL/6 female mice were purchased from Jackson Labs (Bar Harbor, Maine) and housed for 3 weeks without exposure to NP dispersion. Mice were fed a semi-purified diet (D12450B, Research Diet, Inc.) *ad libitum*. After the mice were 9 weeks old, CeO<sub>2</sub>NPs were administered via oral gavage. CeO<sub>2</sub>NPs were introduced during the feeding period at 3 p.m. daily for 10-d. The feeding suspension was made fresh daily and was sonicated for 30 min before gavage. The hydrodynamic size and zeta potential of the feeding suspension were monitored daily to ensure consistency.

Altogether, four dosing scenarios were investigated including control, daily gavage of 4 or 20 µg of 30–50 nm CeO<sub>2</sub>NPs, an equivalent of 0.15 and 0.75 mg/kg body weight/day (T1 and T2), and daily gavage of 20 µg of <25 nm CeO<sub>2</sub>NPs (T3). Unlike most studies, which used high concentrations of CeO<sub>2</sub>NPs to investigate their toxicity, low levels of dosage representing most-likely exposure levels were used in this study. This will help to gain baseline information on the current risks of CeO<sub>2</sub>NPs because these dosages allow us to evaluate the fate and distribution of CeO<sub>2</sub>NPs in relatively healthy populations. Half of the mice from each treatment (n = 12) were sacrificed after 10-d, while the remainder (n = 6) were gavaged with 0.2 mL of DI water daily for another 7-d as a clearance period. Following termination at both the feeding and clearance stages, multiple organs including the liver, heart, spleen, stomach, lung, kidney, brain, and small intestine were collected and weighed to obtain their fresh weight. Mouse feces, blood, and urine were also collected before being sacrificed. Samples were split into two subsamples, which were used for total Ce element analysis and nanoparticle size/concentration analysis.

## 2.3. Total Ce concentration in mouse

Organ tissues used for total Ce analysis were oven dried at 70 °C for 48 h. The dried tissues were then ground into powders, weighed, and acid digested in accordance with the USEPA Method 3050B to determine total Ce content using an inductively-coupled plasma-mass spectrometry (ICP-MS) (Xu et al., 2022; Dan et al., 2016). The blood samples were analyzed shortly after their collection. Briefly, 0.4 mL of whole blood was centrifuged at 1500 g for 10 min after coagulation to obtain the serum, which was then transferred to a clean centrifuge tube and mixed with 1.6 mL of 5% HNO<sub>3</sub>, which was further diluted four times with DI water. The sample was then directly analyzed with ICP-MS for Ce. Urine samples were directly analyzed by ICP-MS without additional pretreatment except for an initial stabilization with 1% HNO<sub>3</sub>.

## 2.4. Nanoparticle concentration and size distribution

Because none of the organ tissues or blood samples after 10-d of feeding contained detectable Ce based on ICP-MS analysis, particle concentration and size distribution of CeO<sub>2</sub>NPs were only performed for feces and urine samples. Specifically, fecal samples were oven-dried at 60 °C overnight, then ground to fine powders using a pestle and mortar. Subsequently, powders (50 mg) from each sample were combined with 5 mL of tetramethylammonium hydroxide (TMAH, 25% w/w) in a pre-cleaned tube and mixed for 30 min at 30 rpm on a rotator. The mixture was then sonicated for 30 min using a water bath sonicator and mixed for an additional 24 h at 30 rpm. Afterwards, 120 mL of ultrapure water

was added to dilute TMAH to 1%, and the sample was stored for 1 h to settle solid residue. The supernatant was withdrawn and diluted with ultrapure water by 50 to 1000 times, which was then sonicated for 15 min right before single particle (SP)-ICP-MS (NexION 2000P, PerkinElmer, Waltham, MA, USA) analysis. Urine samples were diluted by ten times using ultrapure water. The diluted samples were vortex mixed for 30 s, followed by bath sonication for 10 min right before SP-ICP-MS analysis.

Detailed operation and method parameters for SP-ICP-MS are summarized in Table S1. AuNP standard (50 nm) was used to measure the transport efficiency for every experiment, which was ~10%. Dissolved Ce standard (10 mg/L, in 2% HNO<sub>3</sub>) was diluted to different concentrations (0.1–10 µg/L) by 0.1% HNO<sub>3</sub> to establish a calibration curve. Syngistix software with a Nano Application module was used for data collection and processing. The size detection limit of CeO<sub>2</sub>NPs was calculated based on the classical method used in most previous publications (Pace et al., 2012; Lee et al., 2014). Specifically, a threshold criterion of  $\mu + 3\sigma$  (where  $\mu$  and  $\sigma$  are the mean and standard deviation of the blank data set, respectively) was calculated and converted to particle diameter based on the calibration curve. The size detection limit of CeO<sub>2</sub>NPs for SP-ICP-MS was 16 nm.

### 3. Results and discussions

#### 3.1. Nanoparticle characterization

Detailed results on the characterization of CeO<sub>2</sub>NPs are summarized in Fig. 1 and Table 1. Overall, the primary particle size fell within the ranges provided by the vendors, but the size distribution was broader. For example, for the 30–50 nm CeO<sub>2</sub>NPs, the actual dominant sizes were 20–60 nm, and for CeO<sub>2</sub>NPs labeled <25 nm, our result indicate that the dominant size of CeO<sub>2</sub>NPs was in the range of 10–40 nm. CeO<sub>2</sub>NPs from the two sources possessed similar crystalline structure as confirmed by the HR-TEM imaging and selected area electron diffraction patterns of these NPs (Fig. 1). The hydrodynamic diameter and zeta potential of CeO<sub>2</sub>NPs in the feeding suspensions showed that the 30–50 nm CeO<sub>2</sub>NPs were negatively-charged (–47 to –49.6 mV) while the smaller ones were positively-charged (+47.8 mV). Greater aggregation of the positively-charged NPs was observed. The average hydrodynamic size of 30–50 nm and <25 nm CeO<sub>2</sub>NPs in a 10 mg/L of suspension was  $326.4 \pm 17.1$  nm and  $110.8 \pm 0.8$  nm, respectively.

#### 3.2. Accumulation of Ce element in mouse

As expected, the exposure to CeO<sub>2</sub>NPs for 10-d at the selected concentrations has little negative impact on mice. The organ weights from the four treatments were comparable after 10-d of NP feeding (Fig. 2), with no observable alteration or damage to mice organs being noticed. In a previous study, female Wistar rats intraperitoneally administered 300 mg CeO<sub>2</sub>NPs/kg bw (23.2 nm) did not show toxic signs with respect to their body weight or mortality 14-d after the injection. Noticeable impact of CeO<sub>2</sub>NPs was only observed when the dosing concentration reached 2000 mg/kg bw, which is unrealistically-high (Kumari et al., 2014). In addition, both male and female SD rats showed no signs of toxicity, e.g., body weight, and functional observations and blood chemistry following oral exposure with 1000 mg CeO<sub>2</sub>NPs/kg bw (14.2 nm) for 28–29 d (Lee et al., 2020). These results suggest that

CeO<sub>2</sub>NPs at low dosages used in this study are unlikely to cause physiological damages. This provides us a good opportunity to evaluate the possible particle fate (e.g., particle aggregation) and distribution in different organs in healthy mouse.

The total concentration of Ce in all organs and blood samples was below the detection limit of ICP-MS, suggesting that the penetration of CeO<sub>2</sub>NPs through the intestinal epithelium is minimal. This result can be explained by the multiple epithelial barriers that NPs must traverse in order to gain access to the circulatory system and accumulate in other organs. The intestinal epithelium contains well-defined mucosal (mucin secreting epithelial cells) surface sealed by practically impermeable tight junctions (Lee, 2015). Typically, the tight junctions between neighboring epithelial cells constrain the diffusion of hydrophilic macromolecules through the paracellular route. Positively-charged NPs interact closely with mucin, a common protein in the mucosal layer, and can only slowly diffuse across the mucosal layer (Zhang et al., 2021). Therefore, the ability for these particles to reach the epithelial barrier and cross it is low. Negatively-charged particles tend to diffuse faster through the mucosal layer and may enhance the permeability of epithelial membranes, in part by loosening the intercellular tight junctions via the downregulation of phosphorylated claudin-4 protein, the active form of claudin-4 protein which controls the tight junction opening (Wang et al., 2017). Nevertheless, our results indicate that the transmembrane movement of negatively-charged particles with the size used in this study is minimal, likely due to the relatively large particle size compared to the pore sizes of epithelial membranes.

Consistent with our results, Enea et al. (2020) investigated the fate and distribution of 60 nm gold NPs both *in vitro* and in male Wistar rats. They found that systemic absorption of AuNPs was low, with fecal clearance as the predominant pathway of elimination (Enea et al., 2020). However, other studies have reported elevated accumulation of NPs in some organs. The inconsistency in the literature with regard to NP distribution following oral intake might be attributed to two reasons. Firstly, many studies that reported the accumulation of metallic NPs in mice organs after oral intake used highly-soluble NPs such as zinc oxide and silver NPs. The use of ICP-MS or other elemental detection technologies for metal quantification in different organs cannot distinguish NPs versus their dissolved ions. As such, the instrument cannot conclusively measure the systematic absorption of NPs because of metal dissolution. For example, a study with Cu NPs showed that the dissolved ion form of Cu is likely the primary form absorbed following CuONP oral exposure (Lee et al., 2016). This interpretation is supported by the greater dissolution of CuONPs versus Cu microparticles in simulated gastrointestinal fluids. Secondly, almost all studies reporting systemic absorption of NPs after oral intake used small nanoparticles (<12 nm). As an example, daily oral administration of iron oxide NPs to female Wistar rats for 10-d resulted in elevated iron accumulation in the liver and spleen, depending on the surface properties of iron oxide NPs. Negatively-charged iron oxide NPs (7–11 nm) accumulated predominantly in the liver whereas the positively-charged NPs mostly accumulated in the spleen (Fahmy et al., 2021). The biodistribution of these NPs distinguished from iron sulfate, which was mainly accumulated in the kidney. Dumala et al. (2019) studied the distribution of orally-ingested nickel oxide NPs (~12 nm) in Wistar rats (sex unknown) after 28-d of repeated dosing and detected elevated levels of Ni in rat liver, followed by kidney. Interestingly, previous studies have reported size-dependent accumulation of NPs in different organ sites



(De Jong et al., 2008). For example, smaller gold NPs (10 nm) were detected in all organ sites while larger particles tended to accumulate in the liver and spleen only after they enter the circulation system. Therefore, a closer examination of relatively larger nanoparticle oral intake data is needed. Characterization of nanoparticle sizes and size distribution in different organs is also critical. Our results showed that CeO<sub>2</sub>NPs at the size and concentration applied in this study had negligible accumulation in different mouse organs. Therefore, additional studies on the maximum size of NPs that can traverse the intestinal epithelium are needed.

### 3.3. Ce in mouse fecal samples

As expected, mouse oral exposure to CeO<sub>2</sub>NPs resulted in significantly-higher concentrations of element Ce in mouse feces than in the control and Ce concentration in the feces increased with the feeding concentration of CeO<sub>2</sub>NPs (Fig. 3A). Notably, the concentration of Ce in the feces from mice gavaged with <25 nm CeO<sub>2</sub>NPs was significantly higher than those exposed to 30–50 nm CeO<sub>2</sub>NPs at the same concentration, suggesting that positively-charged CeO<sub>2</sub>NPs were cleared faster than the negatively-charged CeO<sub>2</sub>NPs. However, after 7-d of clearance, the Ce concentration in mouse feces are comparable in all treatments including the control (Fig. S1), indicating that it took less than 7-d for mice to clear residual NPs.

The kinetics of clearance is important because NPs retained in the intestine could alter the composition and metabolic function of the gut microbiome, whose role in regulating the integrity of intestinal epithelium has been clearly shown (Zhu et al., 2022). Detailed studies in nanoparticle clearance kinetics and their interactions with gut microbiome in the future will shed light on the potential impact of orally-ingested NPs. The time reported for full clearance after oral intake of CeO<sub>2</sub>NPs ranges from less than 24 h to several weeks in the literature (Casals et al., 2020). This wide range of time needed for clearance could be attributed to the different properties of NPs used in those studies including their concentration, size and surface properties. Thus, more systematic studies with well controlled nanoparticle properties are needed to correlate the fate and biodistribution of orally-taken NPs with their properties.

As shown in Fig. 4, the nanoparticle concentration in the feces was proportional with the feeding concentration for 30–50 nm CeO<sub>2</sub>NPs. Interestingly, the feces from mice exposed to <25 nm CeO<sub>2</sub>NPs (T3) was significantly higher than that from T2 even though the mice in these two groups were exposed to similar concentration of CeO<sub>2</sub>NPs. The mean particle size in the fecal samples from these two treatments were comparable. These results suggest the presence of large numbers of smaller particles and a few large aggregates in the feces from the <25 nm CeO<sub>2</sub>NPs treatment group. The strikingly different particle size distribution in the feces between the two types of NPs suggest the potential for highly distinctive interactions with gut microbiome, which underscores the need to characterize the in different tissues and biological samples after exposure.

### 3.4. Ce in urine samples

Higher concentrations of total Ce element were also detected in the urine samples from mice fed with higher doses of CeO<sub>2</sub>NPs (Fig. 3B). However, the difference was only significant for mice exposed to the smaller and positively-charged CeO<sub>2</sub>NPs. This is likely because of the presence of much smaller CeO<sub>2</sub>NPs in the suspension of <25 nm CeO<sub>2</sub>NPs. To gain more insights, we also analyzed the urine samples using SP-ICP-MS. The SP-ICP-MS did not find significant level of CeO<sub>2</sub>NP larger than the size detection limit (16 nm) in the urine sample. These results suggest that the higher total Ce concentration detected by conventional ICP-MS method in the urine samples dosed with high concentration of <25 nm CeO<sub>2</sub>NP might be present as smaller (<16 nm) size particles. A study using a different type of NPs reported the detection of NPs from the urine samples but stated that only particles that have a hydrodynamic size <5 nm could enter the urinary system (Choi et al., 2007). Our results suggest that even though CeO<sub>2</sub>NPs might be excreted with the urine, this is a minor route of excretion compared with the fecal route.

## 4. Conclusions

In summary, our results demonstrate that orally-ingested CeO<sub>2</sub>NPs at levels typically found in commercial products or at slightly higher projected levels did not lead to overt toxicity to healthy mice. Their limited accumulation in mice organs was probably due to the protective role of intestinal epithelial barrier. This may justify the use of CeO<sub>2</sub>NPs as nanocarriers because of the low risk of long term accumulation of NPs if the size of CeO<sub>2</sub>NPs can be controlled above a certain threshold. However, it should be cautioned that engineered NPs may still pose risks to those who suffer from “leaky” gut, which requires additional investigation. On the other hand, if CeO<sub>2</sub>NPs are used as a component of nanomedicine, oral administration may not be an effective delivery method unless NPs are reduced to much smaller size (at least smaller than 12 nm). Our results also show that surface charge affects the fate, distribution and clearance time of orally-taken NPs. Therefore, manipulation of nanoparticle size and surface properties can be an effective approach to alter the fate and distribution of NPs to achieve the goal of its use.

## Supplementary Material

Refer to Web version on PubMed Central for supplementary material.

## Acknowledgements

Funding was provided by the Allen Endowed Chair in Nutrition & Chronic Disease Prevention, Texas A&M AgriLife Research, and the National Institutes of Health (R35-CA197707 and P30-ES029067).

## References

- Baldir V, Bedioui F, Mignet N, Margail I, Berret J-F, 2018. The enzyme-like catalytic activity of cerium oxide nanoparticles and its dependency on Ce<sup>3+</sup> surface area concentration. *Nanoscale* 10 (15), 6971–6980. [PubMed: 29610821]
- Casals E, Zeng M, Parra-Robert M, Fernández-Varo G, Morales-Ruiz M, Jiménez W, Puentes V, Casals G, 2020. Cerium oxide nanoparticles: advances in biodistribution, toxicity, and preclinical exploration. *Small* 16 (20), 1907322.



- Chazelas E, Deschasaux M, Srouf B, Kesse-Guyot E, Julia C, Alles B, Druésne-Pecollo N, Galan P, Hercberg S, Latino-Martel P, 2020. Food additives: distribution and co-occurrence in 126,000 food products of the French market. *Sci. Rep.* 10 (1), 1–15. [PubMed: 31913322]
- Choi HS, Liu W, Misra P, Tanaka E, Zimmer JP, Ipe BI, Bawendi MG, Frangioni JV, 2007. Renal clearance of nanoparticles. *Nat. Biotechnol.* 25 (10), 1165. [PubMed: 17891134]
- Dan Y, Ma X, Zhang W, Liu K, Stephan C, Shi H, 2016. Single particle ICP-MS method development for the determination of plant uptake and accumulation of CeO<sub>2</sub> nanoparticles. *Anal. Bioanal. Chem.* 408 (19), 5157–5167. [PubMed: 27129977]
- De Jong WH, Hagens WI, Krystek P, Burger MC, Sips AJ, Geertsma RE, 2008. Particle size-dependent organ distribution of gold nanoparticles after intravenous administration. *Biomaterials* 29 (12), 1912–1919. [PubMed: 18242692]
- Dekkers S, Krystek P, Peters RJ, Lankveld DP, Bokkers BG, van Hoeven-Arentzen PH, Bouwmeester H, Oomen AG, 2011. Presence and risks of nanosilica in food products. *Nanotoxicology* 5 (3), 393–405. [PubMed: 20868236]
- Dumala N, Mangalampalli B, Kalyan Kamal SS, Grover P, 2019. Repeated oral dose toxicity study of nickel oxide nanoparticles in Wistar rats: a histological and biochemical perspective. *J. Appl. Toxicol.* 39 (7), 1012–1029. [PubMed: 30843265]
- Enea M, Pereira E, Silva DD, Costa J, Soares ME, de Lourdes Bastos M, Carmo H, 2020. Study of the intestinal uptake and permeability of gold nanoparticles using both in vitro and in vivo approaches. *Nanotechnology* 31 (19), 195102. [PubMed: 31962292]
- Fahmy HM, Abd El-Daim TM, Ali OA, Hassan AA, Mohammed FF, Fathy MM, 2021. Surface modifications affect iron oxide nanoparticles' biodistribution after multiple-dose administration in rats. *J. Biochem. Mol. Toxicol.* 35 (3), e22671. [PubMed: 33295111]
- He X, Zhang H, Shi H, Liu W, Sahle-Demessie E, 2020. Fates of Au, Ag, ZnO, and CeO<sub>2</sub> nanoparticles in simulated gastric fluid studied using single-particle-inductively coupled plasma-mass spectrometry. *J. Am. Soc. Mass Spectrom.* 31 (10), 2180–2190. [PubMed: 32881526]
- Inbaraj BS, Chen B-H, 2020. An overview on recent in vivo biological application of cerium oxide nanoparticles. *Asian J. Pharm. Sci.* 15 (5), 558–575.
- Kumari M, Kumari SI, Kamal SSK, Grover P, 2014. Genotoxicity assessment of cerium oxide nanoparticles in female Wistar rats after acute oral exposure. *Mutat. Res. Genet. Toxicol. Environ. Mutagen* 775, 7–19. [PubMed: 25435351]
- Lamas B, Martins Breyner N, Houdeau E, 2020. Impacts of foodborne inorganic nanoparticles on the gut microbiota-immune axis: potential consequences for host health. *Part. Fibre Toxicol.* 17 (1), 1–22. [PubMed: 31900181]
- Lee I-C, Ko J-W, Park S-H, Shin N-R, Shin I-S, Moon C, Kim J-H, Kim H-C, Kim J-C, 2016. Comparative toxicity and biodistribution assessments in rats following subchronic oral exposure to copper nanoparticles and microparticles. *Part. Fibre Toxicol.* 13 (1), 1–16. [PubMed: 26746196]
- Lee J, Jeong J-S, Kim SY, Lee S-J, Shin Y-J, Im W-J, Kim S-H, Park K, Jeong EJ, Nam S-Y, 2020. Safety assessment of cerium oxide nanoparticles: combined repeated-dose toxicity with reproductive/developmental toxicity screening and biodistribution in rats. *Nanotoxicology* 14 (5), 696–710. [PubMed: 32301357]
- Lee SH, 2015. Intestinal permeability regulation by tight junction: implication on inflammatory bowel diseases. *Intestinal research* 13 (1), 11. [PubMed: 25691839]
- Lee S, Bi X, Reed RB, Ranville JF, Herckes P, Westerhoff P, 2014. Nanoparticle size detection limits by single particle ICP-MS for 40 elements. *Environ. Sci. Technol.* 48 (17), 10291–10300. [PubMed: 25122540]
- McClements DJ, Xiao H, 2017. Is nano safe in foods? Establishing the factors impacting the gastrointestinal fate and toxicity of organic and inorganic food-grade nanoparticles. *npj Science of Food* 1 (1), 1–13. [PubMed: 31304243]
- Medina-Reyes EI, Rodríguez-Ibarra C, Déciga-Alcaraz A, Díaz-Urbina D, Chirino YI, Pedraza-Chaverri J, 2020. Food additives containing nanoparticles induce gastrotoxicity, hepatotoxicity and alterations in animal behavior: the unknown role of oxidative stress. *Food Chem. Toxicol.* 146, 111814. [PubMed: 33068655]

- Pace HE, Rogers NJ, Jarolimek C, Coleman VA, Gray EP, Higgins CP, Ranville JF, 2012. Single particle inductively coupled plasma-mass spectrometry: a performance evaluation and method comparison in the determination of nanoparticle size. *Environ. Sci. Technol.* 46 (22), 12272–12280. [PubMed: 22780106]
- Pinget G, Tan J, Janac B, Kaakoush NO, Angelatos AS, O’Sullivan J, Koay YC, Sierro F, Davis J, Divakarla SK, 2019. Impact of the food additive titanium dioxide (E171) on gut microbiota-host interaction. *Front. Nutr.* 6, 57. [PubMed: 31165072]
- Wang J, Kong M, Zhou Z, Yan D, Yu X, Cheng X, Feng C, Liu Y, Chen X, 2017. Mechanism of surface charge triggered intestinal epithelial tight junction opening upon chitosan nanoparticles for insulin oral delivery. *Carbohydr. Polym.* 157, 596–602. [PubMed: 27987967]
- Xu L, Wang X, Shi H, Hua B, Burken JG, Ma X, Yang H, Yang JJ, 2022. Uptake of engineered metallic nanoparticles in soil by lettuce in single and binary nanoparticle systems. *ACS Sustain. Chem. Eng.* 10, 16692–16700.
- Zhang Y, Xiong M, Ni X, Wang J, Rong H, Su Y, Yu S, Mohammad IS, Leung SSY, Hu H, 2021. Virus-mimicking mesoporous silica nanoparticles with an electrically neutral and hydrophilic surface to improve the oral absorption of insulin by breaking through dual barriers of the mucus layer and the intestinal epithelium. *ACS Appl. Mater. Interfaces* 13 (15), 18077–18088. [PubMed: 33830730]
- Zhu X, Li H, Zhou L, Jiang H, Ji M, Chen J, 2022. Evaluation of the gut microbiome alterations in healthy rats after dietary exposure to different synthetic ZnO nanoparticles. *Life Sci*, 121250 [PubMed: 36455650]

**HIGHLIGHTS**

- CeO<sub>2</sub>NPs at current exposure levels pose low risks after oral intake by mice.
- Orally-ingested CeO<sub>2</sub>NPs >25 nm are unlikely to accumulate in mouse organs.
- Fecal discharge is the dominant pathway of clearance for orally-ingested CeO<sub>2</sub>NPs.
- Clearance of orally-exposed CeO<sub>2</sub>NPs takes <7-d.

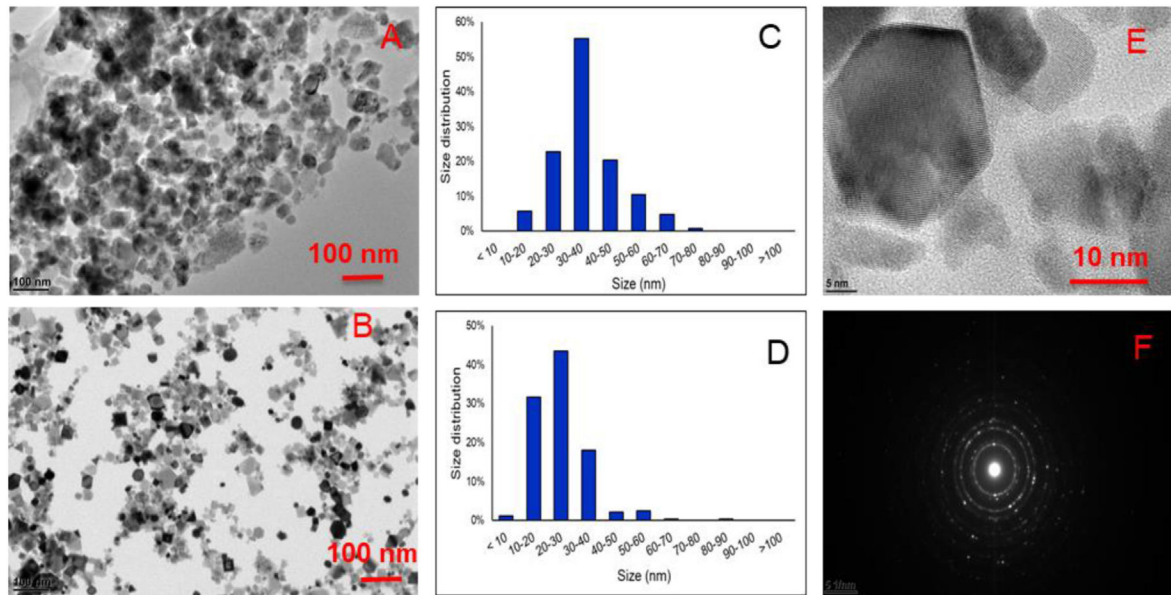


**Fig. 1.** Transmission electron microscopic (TEM) images of two types of CeO<sub>2</sub>NPs, 30–50 nm (A) and 25 nm (B), nanoparticle size distributions of two types of CeO<sub>2</sub>NPs obtained from ImageJ analysis (CD), high resolution TEM image of 30–50 nm CeO<sub>2</sub>NPs (E) and selected area diffraction (SEAD) pattern of 30–50 nm CeO<sub>2</sub>NPs (F).

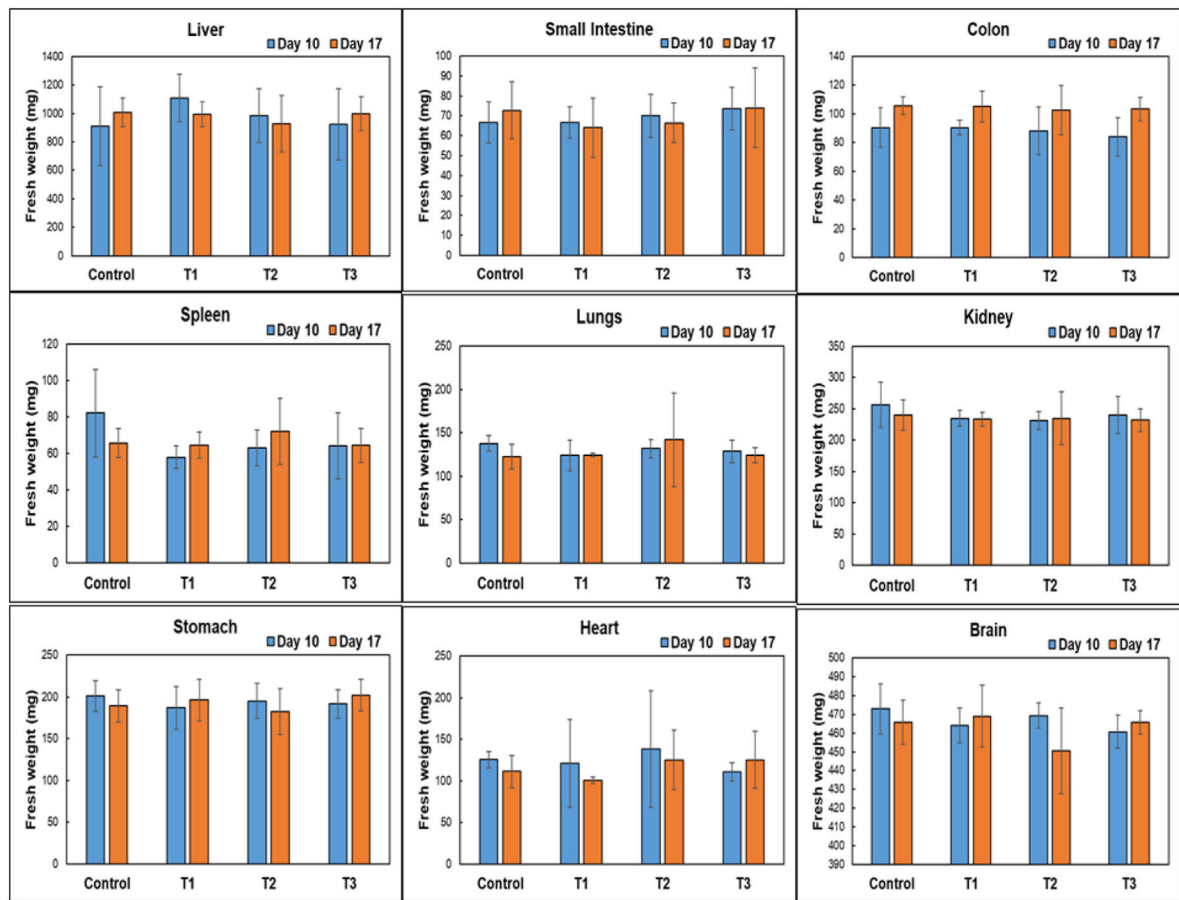


**Fig. 2.** Mouse organ weights collected after 10-d of continuous gavage of CeO<sub>2</sub>NPs suspensions and following 7-d of clearance. T1 and T2: oral administration of 200  $\mu$ L of 20 mg/L and 100 mg/L of CeO<sub>2</sub>NPs (30–50 nm), respectively, daily for 10-d, T3: oral administration of 200  $\mu$ L of 100 mg/L of CeO<sub>2</sub>NPs (<25 nm) daily for 10-d. Control mice were gavaged with 200  $\mu$ L of water daily.

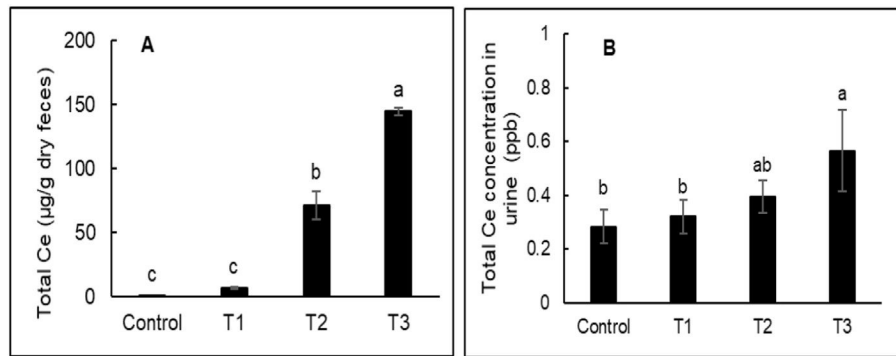


**Fig. 3.** Total cerium concentration in the feces (A) and urine (B) samples after 10-d of continuous gavage. T1 and T2: oral administration of 0.2 mL of 20 mg/L and 100 mg/L of CeO<sub>2</sub>NPs (30–50 nm), T3: oral administration of 0.2 mL of 100 mg/L of CeO<sub>2</sub>NPs (<25 nm). Control mice were gavaged with 0.2 mL of water daily and bars represent standard deviation (n = 5).



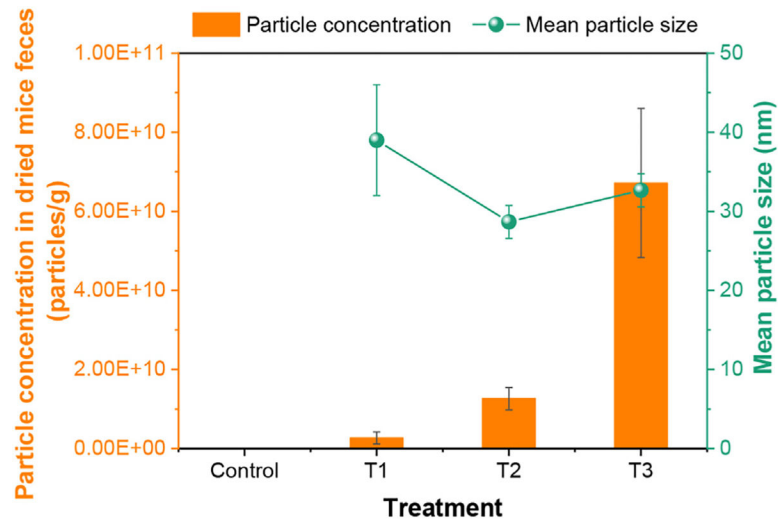


**Fig. 4.** Nanoparticle concentration and mean particle size in the feces after 10-d of continuous gavage. T1 and T2: oral administration of 0.2 mL of 20 mg/L and 100 mg/L of CeO<sub>2</sub>NPs (30–50 nm), and T3: oral administration of 0.2 mL of 100 mg/L of CeO<sub>2</sub>NPs (<25 nm). Control mice were gavaged with 0.2 mL of water daily.

**Table 1**

Summary of the properties of CeO<sub>2</sub>NPs in different treatment solutions.

Treatment	T1	T2	T3
Concentration	20 mg/L	100 mg/L	20 mg/L
Primary particle size distribution *	30–50 nm	30–50 nm	<25 nm
Dominant particle size distribution &	20–60 nm	20–60 nm	10–40 nm
Hydrodynamic size	313.8 ± 9.1 nm	326.4 ± 17.1 nm	110.8 ± 0.8 nm
Zeta potential	-47.0 ± 1.6 mV	-49.6 ± 0.7 mV	+47.8 ± 2.2 mV
pH	5.21 ± 0.24	5.99 ± 0.18	4.54 ± 0.09

\*: provided by the vendor,

&: measured in this study.

Author Manuscript

Author Manuscript

Author Manuscript

Author Manuscript